

High-Efficiency Cell Concepts on Low-Cost Silicon Sheets

R.O. Bell and K.V. Ravi
Mobil Solar Energy Corporation
Waltham, Massachusetts 02254

N85-31621

INTRODUCTION

The strongest leverage for reducing the cost of power generated from solar energy is the efficiency of the solar cell. It is easy to see that given a target cost for electrical energy there is a minimum solar efficiency that must be exceeded even if the module cost becomes negligible. This arises because of the balance of systems cost (land, support structures, power conditioning, wiring, etc.). For example, for competition with an intermediate load coal-fired plant, a module efficiency of above 10% must be maintained [1]. As this minimum efficiency is exceeded, the power costs fall rapidly.

Thus, the drive to produce high efficiency solar cells is very strong. If the technology does not have the potential for realizing this minimum value, then it will be non-competitive for the particular scenario projected.

In this paper we will discuss the limitations on sheet growth material (primarily with reference to EFG) in terms of the defect structure and minority carrier lifetime. Using simple models for material parameters and behavior of solar cells, we will estimate what effect these various defects will have on performance. Given these limitations we can then propose designs for a sheet growth cell that will make the best of the material characteristics.

When discussing solar cells, the material is often characterized in terms of a diffusion length, L_p , whose square is directly proportional to the lifetime, τ , i.e., $L_p^2 = D\tau$, where the constant D is the diffusion coefficient. For a homogeneous material the diffusion length is also a measure of the distance over which minority carriers are collected. For inhomogeneous material where the scale of the lifetime variations may be less than the local diffusion length, the meaning of the diffusion length as a collection distance breaks down.

When techniques such as SPV or spectral response measurements are applied to measure diffusion lengths in inhomogeneous material, it must be kept in mind that the derived quantity, while often referred to as a diffusion length, is really a charge collection distance. It is a complex average depending on how the minority carrier lifetime varies with position. Generally it is clear from the context if we are using diffusion length as a measure of local lifetime or as a charge collection distance.

PRECEDING PAGE BLANK NOT FILMED

I. DEFECTS

The primary defects in silicon that show electrical activity, i.e., contribute to the majority carrier concentration or act as recombination centers, are dislocations, grain boundaries, twins, inclusions including SiC and silicates, point defects of either a substitutional or interstitial character and impurities such as transition metals and oxygen and carbon [2]. There are other closely related defects such as swirls, stacking faults, partial dislocations, etc., but in this paper we will concentrate our remarks on the more general types listed above.

F. Wald has recently presented a comprehensive review of defects in EFG silicon with a discussion of the type and number of defects [2]. Rather than including figures illustrating the defects, we will simply reference his paper.

A. Dislocations

The classic edge dislocation, which can be visualized as being formed by removing an atomic half plane, should exhibit a single line of silicon atoms whose bonding requirements are not satisfied. In a simple minded picture, a dislocation would exhibit a series of dangling bonds, one of which is associated with each plane. If each of these atoms behaved as a recombination center, then for a dislocation density of 10^5 cm^{-2} with a typical cross-section of 10^{-15} cm^{-2} , the lifetime would be of the order of 30 μsec which corresponds to a 300 μm diffusion length in p-type material.

In actual fact most of the broken bonds will be reconstructed [2] so the number of "dangling bonds" will be substantially less, thus giving a much lower potential for recombination.

Another possibility might be that recombination occurs not at dangling bonds but rather at an impurity cloud attracted to the dislocations. If more than one electrically active atom were associated with each atomic lane, then the potential diffusion length could be reduced. We should note, though, that as will be discussed in Section IIB, having the electrically active recombination centers concentrated around the dislocations may actually result in a higher efficiency cell than if the same total number of impurities were uniformly distributed throughout the solid.

B. Grain Boundaries

When two grains with different orientations intersect, they form a grain boundary. First order and higher order twins can be considered a sub-class of grain boundaries. In the general case, grain boundaries can be constructed from a series of edge and screw dislocations. In twins a specific orientation between the grains exists, but for general grain boundaries this is not necessary.

A convenient way to observe the electrical/recombination activity of dislocations and grain boundaries is by the use of EBIC. By making line scans perpendicular to the grain boundaries their recombination properties can be characterized typically in terms of a recombination velocity, v_r , and diffusion length, L_p [3,4]. Optical techniques, LBIC, have also been used in a similar

fashion to obtain the same material characteristics [4]. Velocities up to 10^5 cm/sec have been observed with typical velocities for "strong boundaries" being the order of 10^4 cm/sec. For such a velocity, the effective grain boundary width ($L_n = 100 \mu\text{m}$, $\alpha = 1000 \text{ cm}^{-1}$) is about $5 \mu\text{m}$. The concept of an effective grain boundary width is due to Zook, and is defined as the equivalent width of a region from which no charge is collected. If we have a high density of strong boundaries ($10^2/\text{cm}$), the loss in short circuit current can become significant (5%). By no means do all grain boundaries have high recombination, and in fact many are electrically very weak or invisible.

Also of importance is the contribution that grain boundary recombination can make to the reverse saturation current. A reduction of 5% in the current collected corresponds to a decrease in the diffusion length by 35% for a homogeneous distribution of recombination centers. This would reduce the reverse saturation current also by 35% and produce a decrease in open circuit voltage of about 10 mV.

Grain boundary recombination can be important if the density of electrically active boundaries is high. Only in the case of small grain size such as produced by CVD or in silicon with a very high intragranular diffusion length will they dominate performance.

C. Inclusions

The principal effect of inclusions is either to physically block the light or to shunt the junction. Typically, inclusions are found to be SiC or silicates. The contribution an ideal shunting particle makes to reverse leakage depends on its diameter and the sheet resistivity of the surface layer to which the shunting occurs. It is easy to show that for a circular shunt of radius, a , and sheet resistivity, ρ_{\square} , the voltage drop, ΔV , for a distance, d , away from the particle is

$$\Delta V = \frac{\rho_{\square} I_{sc}}{2} [d^2(\ln(d/a) + 1/2) - a^2/2] \quad (1)$$

For a typical I_{sc} of 30 mA/cm^2 , ΔV of 0.25V , ρ_{\square} of $50 \Omega/\square$, the current not collected (which is equal to $\pi d^2 I_{sc}$) is about 5 mA/particle . In most cases the finite resistivity of the SiC limits the current to less than that predicted by Eq. (1). The SiC density is generally less than one per cm^2 , and experimentally it is observed that such shunting is rarely a problem.

In the unfortunate case, though, that the metallization covers the inclusion, the cell will be almost completely shunted since in this case ρ_{\square} is very small (the order of $5 \text{ m}\Omega/\square$). Since only about 5% of the solar cell is metallized, this is a rare occurrence.

The fractional volume of a silicate particle is so small and the resistivity is so high that any contribution to losses by light blockage or shunting can probably be safely ignored.

Measurements of the junction characteristics of EFG solar cells often show a contribution to the reverse saturation current that has a temperature

dependence characteristic of tunneling rather than space charge recombination [5]. It has been suggested that this phenomenon could be due to very small precipitates that introduce charge centers into the space charge region. The loss in efficiency shows up as a soft knee and is easily measured using the dark I-V characteristic.

D. Point Defects and Impurities

So far the discussion has dealt with defects that are visible, at least under moderate magnification with an optical microscope or in an SEM. Point defects and impurities in sheet silicon are those that occupy either a single or a few lattice sites and cannot generally be directly imaged. The defects may be native, such as self interstitials or vacancies, metallic, such as Fe, Ti, Mn, etc., or non-metallic, such as carbon and oxygen. Dopants such as B and P are in a sense substitutional defects.

In order for a point defect or impurity to significantly affect the minority carrier lifetime (for the sake of definiteness we will talk about electrons in p-type material), its energy level must be located above the quasi-Fermi level for electrons, but not so near the conduction band edge that any trapped carriers can easily be excited [6]. Shockley-Read-Hall (SRH) theory predicts that the most efficient recombination centers are located at the center of the energy gap.

A large number of elements have been found to produce centers in the band gap of silicon. Their characteristics have been the subject of a number of publications, including those by Weber [7], Sze [8] and Schibli and Milnes [9]. The density of the centers must be high enough such that the probability of trapping a charge is significant. For a 1 μ sec lifetime with a reasonable cross-section (10^{-15} cm²), the trapping center density should be 10^{14} cm⁻³, which is a very small number in terms of chemical concentration.

Thus, it is natural to expect that inadvertent contamination can drastically reduce the lifetime in silicon. In fact, it is surprising how tolerant EFG is to the level of metallic impurities. Typically impurity levels range from one to 10 ppm and have little correlation with cell performance. There is apparently a major difference between the total impurity content and those that contribute to recombination. Experiments [2,10] show that the introduction of Fe and Mo at concentrations up to 5×10^{13} cm⁻³ can be tolerated.

Besides the metallic impurities, other species such as carbon and oxygen are present in large quantities. The carbon comes from the crucible (if graphite) and die material, and the oxygen from the crucible (if fused quartz) and gaseous ambient. Individual carbon atoms in a silicon lattice are not electrically active but probably express their activity because of interactions with other defects. Oxygen when interstitial is not electrically active, but under various heat treatments forms complexes that act as donors or recombination centers.

Oxygen has been shown to play an important role in producing EFG silicon with the longest diffusion length [11]. The oxygen can be introduced either from the ambient or from the crucible. The diffusion length for oxygenated EFG

silicon is not only higher than in EFG without additional oxygen at low light levels, but also it shows a stronger dependence on illumination level.

In non-degenerate silicon, including CZ, float zone, EFG, etc., the lifetime is dominated by an SRH recombination process. This lifetime is generally found to decrease rapidly with doping density. Fuller [12] and Fossum et al. [13,14] have modeled the defect density as if it were a chemical reaction driven by the doping density. The lifetime, τ , can be approximated to depend on the doping level, N_D , as

$$\tau = \tau_0 / (1 + N_D/N_0) \quad (2)$$

where τ_0 is a constant that is a function of material quality. This is the expression used by Rohatgi and Rai-Choudhury [15] when modeling high efficiency solar cells. For N_0 they use $7 \times 10^{15} \text{ cm}^{-3}$.

In one EFG experiment in which the boron concentration was varied to give resistivities between 0.2 and 10 $\Omega\text{-cm}$, the data can be approximately fit with τ_0 having a value of 0.7 μsec [2,16]. By contrast the Auger recombination, even in high quality material, does not dominate until the resistivity is below 0.1 $\Omega\text{-cm}$. Other EFG material has been grown with a diffusion length of over 150 μm at 4 $\Omega\text{-cm}$ which would imply a value of τ_0 of 10 μsec .

II. SOLAR CELL PERFORMANCE

A good deal of work has been devoted to modeling the behavior of solar cells but mostly on homogeneous material (both with respect to depth and areal distribution). With ribbon material this is not necessarily a good assumption and at times the effect of inhomogeneous distributions of minority recombination centers, crystalline defects and majority carrier doping cannot be neglected.

In this section we model the behavior of an EFG solar cell to determine how to get the most out of it. An outline of the technique is given in the Appendix. It is similar to the approach suggested by Wolf [17] and can include surface recombination, doping dependent lifetimes including Auger and SRH, and band gap narrowing. Calculations based on the solution of the diffusion equation, including electric fields produced by doping gradients, give similar results when applied to the same cases modeled here.

In the first part of this section we calculate the charge generation and collection distributions produced by the solar spectrum. Next we discuss some aspects of inhomogeneous distributions of lifetime and effect on solar cells. Finally, the effect of resistivity and surface passivation is considered.

Of course, as when attempting to extract the highest possible efficiency from any cell, it is important that the metal coverage be as little as possible consistent with a low series resistance and that any anti-reflection coating be optimized whether one or two layers. Because sheet growth materials, except for web, generally do not have a predetermined orientation, surface etching to produce faceting is not an option, although growth using a corrugated die to produce an equivalent effect may be possible.

A. Charge Generation Rate

Figure 1 shows a plot of the charge generation rate for an AM1.5 [18] spectrum in silicon [19]. By far the highest generation rate is close to the surface. If we integrate this curve and normalize it relative to the total possible hole electron pairs produced (Fig. 2), we see that 50% of the possible charge is generated within 5 μm of the surface and 90% within 150 μm .

There is quite a long tail on the optical absorption so even though most charge is generated relatively near the surface, if we want to collect almost all minority carriers (95 to 99%) a very long diffusion length (the order of 1000 μm) would be required.

B. Areal Inhomogeneities

Calculations have been made of the effect of areal lifetime inhomogeneities on solar cells. In general the regions with a low lifetime dominate the performance, both by the effect on short circuit current and open circuit voltage [20]. Although this result might, at first reading, seem to indicate that a homogeneous material is best, it can be shown through simple arguments that when the total number of recombination centers is held fixed, an inhomogeneous distribution can produce a cell with a higher efficiency than one in which the centers are uniformly distributed [21]. Thus, what at first glance might be considered a disadvantage of sheet grown silicon can really be an advantage. Assuming that the behavior of recombination centers is independent of concentration, if the recombination centers are concentrated in a few small regions, then the performance may be improved.

Figure 3 shows a plot of the relative efficiency as a function of the amount of poor area. Depending upon the ratio of the number of recombination centers in the poor area to the good area, the maximum efficiency occurs when the poor area occupies between 10 and 30% of the total cell area. Obviously it is better if the total number of impurities or recombination centers can be minimized, but if they are present it is desirable that they be segregated rather than uniformly distributed.

C. Optimum Resistivity

High efficiency solar cells have been made using either moderate resistivity silicon with a long lifetime or low resistivity with a moderate lifetime material. Recently, Green [22] has analyzed the effect of Auger recombination on the open circuit voltage and efficiency and concludes that for heavily and lightly doped material, Auger recombination places the most stringent limitation on solar cell performance. He estimates a maximum open circuit voltage of about 720 mV for "thick" cells. As we have seen in Section IID, the observed practical lifetime limit of the base is not Auger but is probably related to a defect/dopant interaction.

Figure 4 shows a plot of the calculated efficiency assuming that the lifetime is given by Eq. (2) with τ_0 of 1 and 10 μsec . The parameters of the n^+ region have been adjusted so that they do not contribute to losses of the solar cell. Clearly a 15% efficient solar cell can be made for the larger value of τ_0 but not for the lower value.

D. Surface Passivation

In the analysis made above, it was assumed that the the surface was well passivated, i.e., recombination was negligible. Much recent work demonstrates the importance of the correct treatment of the n^+ region if the maximum is to be obtained from solar cells [15,23,24]. With a base lifetime of 10 μ sec, the effective recombination velocity, $v_s = D/L$, must be less than about 2×10^5 cm/sec. To be base limited requires that the contribution from the emitter, including surface and material recombination, must be less than that

Techniques have been developed for passivating both float zone and CZ [15,24]. There is no reason to believe that they cannot be applied to sheet grown materials. At the doping levels used in the n^+ layer, Auger limitations on the lifetime should be dominant even in relatively low quality material. Auger recombination varies like the square of the doping density, whereas defect/doping recombination varies directly with doping density. This means that at high enough doping the ultimate limitation will be Auger. The inherent built-in electric fields produced during any diffusion process, especially for shallow junctions, will minimize emitter recombination.

III. SUMMARY

The optimum EFG cell will have the highest doping consistent with the defect/doping limit on lifetime. It probably will be below 1 Ω -cm. The junction depth will be shallow with a sheet resistivity of at least 100 Ω/\square . Green et al. [23] have shown that the sheet resistivity needs to be above 100 Ω/\square if the recombination is to be dominated by the surface rather than the bulk properties of the n^+ region.

The thickness of the base will probably be determined by the ability to handle thin sheets rather than the requirement for any back surface field. With modest diffusion lengths, the gain in efficiency with back surface fields is not important until the substrates are so thin that practical handling problems rule out their use. For example, the peak efficiency for a 100 μ m diffusion length BSF cell, peaks at a sample thickness of about 60 μ m, but it is only about 8% better than a thick ($> 300 \mu$ m) solar cell.

Another critical aspect is to control the lifetime of the finished cell. Post fabrication techniques have been developed, such as hydrogen passivation, to improve material quality after fabrication [25]. This works well even though only a relatively thin region is affected because the open circuit voltage and fill factor are controlled to a large extent by the material properties very close to the surface.

IV. CONCLUSION

The achievement of high cell efficiencies in sheet silicon, grown at high rates and prone to contain significant densities of imperfections and impurities, requires developments in both crystal growth technology and cell processing approaches. Variations in crystal growth of importance include control over defect structure and impurity content. Key developments include the following:

- (a) Control over impurity content in crystal growth from the melt is needed to decrease the number of lifetime reducing impurities. In the case of EFG, this includes appropriate purification of elements of the crystal growth machine.
- (b) Control over defect structure and density is needed to minimize defect-impurity interactions. Areas of interest here include reduction in plastic deformation as a consequence of post-growth heat treatment and the minimization of residual stress. In this context, it is preferable to increase the area rate of production by the growth of wide crystals grown at moderate linear growth rates than by increasing linear growth rates, since defect generation by plastic deformation in response to thermo-elastic and thermo-plastic stresses appears to be a stronger function of linear growth rates than of the crystal width.
- (c) The influence and role of carbon in silicon continues to be an unknown quantity. A better understanding of the influence of carbon (and oxygen) on electrical phenomena in silicon is needed.

Device processing implications are many. The key ones have been touched upon in this paper. The fundamental issue is one of achieving the optimum synergy between base material quality and device processing variables. At the current stage of development of low-cost silicon sheet technologies, a strong coupling between material quality, and thus the variables during crystal growth, and device processing variables exists. The challenges are twofold: (1) the optimization of this coupling for maximum performance at minimal cost, and (2) a decoupling of materials from processing by continual improvement in base material quality to make it less sensitive to processing variables.

Appendix - Solar Cell Efficiency Calculation

A number of different schemes to model solar cells have been developed over the years since Prince [26] showed how cell efficiency varied with band gap. Probably the most accurate and mathematically rigorous is that by Hauser and co-workers [27,28]. They solve the fundamental device equations but the procedure is complicated and requires large amounts of computer time. Other first order models such as the use of a shifted diode curve, a typical example being Wysocki and Rappaport [29], do not generally allow for inclusion of effects such as electric fields, heavy doping and back surface fields.

Recently though, Wolf [17,30] has suggested a technique which relies on the simplicity of the diode model but allows inclusion of heavy doping effects by the concept of a so-called transport velocity. This idea was introduced by Gunn [31] for the study of carrier accumulation associated with semiconductor junctions. Bowler and Wolf [17] have used the technique to make estimates of the ultimate efficiency of solar cells and how they depend on various geometrical and material parameters.

We have adapted their procedure to examine what might be expected for EFG material. The transport velocity concept was combined with models of charge generation and collection to look at the solar cell output parameters.

Theory

As shown by Gunn [31], for p-type material the diode current at any position, $j(x)$, can be expressed by

$$j(x) = qn(x)u(x) \quad (A1)$$

where $n(x)$ is the minority carrier density, $u(x)$ is the transport velocity, and q is the electronic charge.

If the diffusion coefficient, D , and minority carrier diffusion length, L , are constant over a region between x and x' , $u(x)$ transforms such that

$$u(x) = \frac{D}{L} \left[\frac{\frac{n(x')L}{D} + \tanh \frac{x-x'}{L}}{1 + \frac{n(x')L}{D} \tanh \frac{x-x'}{L}} \right] \quad (A2)$$

Thus, if we know the value of u at some position x' , then with Eq. (A2) we can calculate it at x . If the various parameters are not constant, then the region can be divided up into steps such that the variation is small over any given region and repeated applications of Eq. (A2) can be used. Note that as $(x - x')$ becomes large compared to L , $u(x)$ goes to D/L .

The transformation for a high/low junction (a change in carrier concentration such as at a p/p^+ or n/n^+ junction) is

$$u(x^+) = \frac{p^+}{p^-} u(x^-) \quad (A3)$$

At the junction, $n(x_j)$ is determined by the barrier height, V , such that

$$n(x_j) = \frac{n_i^2}{p} [\exp(qV/kT) - 1] \quad (A4)$$

where n_i is the intrinsic carrier concentration.

Combining Eqs. (A1) and (A4) at the junction and using the light generated current, j_{sc} , to offset the diode equation, we obtain

$$j = j_0 [\exp(qV/kT) - 1] + j_{sc} \quad (A5a)$$

$$j_0 = q \frac{n_i^2}{p} u(x_j) \quad (A5b)$$

A similar treatment will give the contribution from the n region. Also, to account for recombination in the space charge region, a term of the form $j_0' [\exp(qV/2kT) - 1]$, where $j_0' = qn_i W/\tau$ is added to Eq. (A5a). W is the width of the space charge region and $\tau = L^2/D$ is the lifetime.

Thus, to model a solar cell, we divide it up into regions where the properties are uniform. Starting with a value for the surface recombination velocity, S , where $u(x) = S$, we apply either Eq. (A2) or (A3) repeatedly until we have arrived at the junction with a value of $u(x_j)$. We next calculate j_{sc} with an expression of the form

$$j_{sc} = q \int_0^{\lambda_{min}} (1 - R(\lambda)) \phi(\lambda) Q(\lambda) d\lambda \quad (A6)$$

where $\phi(\lambda)$ is the flux for the desired spectrum (here we have used AM1.5 [11] normalized to 100 mW/cm²), $Q(\lambda)$ is the charge collection discussed below and $R(\lambda)$ is the reflectivity at the front surface. The contributions from the space charge region and the surface n^+ layer also are added to j_{sc} .

The solar cell is now characterized by Eq. (A5) where j_0 , j_0' and j_{sc} depend on material and geometrical parameters. Because of surface coverage by the metal grid and optical losses in the AR coating, $R(\lambda)$ is not zero. For simplicity, in the calculation $R(\lambda) = 0.15$ was used for all wavelengths. The peak power, P_m , is given by $d(jV)dV = 0$ and the open circuit voltage $j(V_{oc}) = 0$, both of which expressions were evaluated numerically. The fill factor, FF, is

$$FF = P_m / V_{oc} j_{sc} \quad (A7)$$

A couple of other items must also be included. At high carrier concentrations, Auger and defect/doping recombination becomes important and their effect on lifetime is included. D also depends on carrier concentration. Through band gap narrowing, n_i varies at high doping levels. Appropriate models for these dependencies were used.

Calculation of $Q(\lambda)$

The basic equations governing the flow of minority carriers in a semiconductor are the current equation and charge continuity equation [19], which in one dimension are

$$j_n = q \mu_n E + q D \frac{\partial n}{\partial x} \quad (A8)$$

$$\frac{\partial n}{\partial t} = U + G + \frac{1}{q} \frac{\partial j_n}{\partial x} \quad (A9)$$

U is the net recombination rate and normally is set equal to n/τ . At equilibrium where $\partial n/\partial t = 0$ and with no electric field, i.e., $E = 0$, by substituting Eq. (A8) into (A9) we obtain the diffusion equation

$$qD \frac{d^2 n}{dx^2} - \frac{n}{\tau} + G = 0 \quad (A10)$$

G is the optical generation term. For the geometry shown in Fig A1, where light can reflect off the back surface, G will be

$$G = \alpha[\exp(-\alpha x) + R \exp(\alpha(x - 2d))] \quad (A11)$$

where R is the reflectivity of the back surface.

We use the general boundary conditions that the carrier concentration is zero at the front junction and that the current, including surface recombination, is continuous at $x = d$

$$n = 0 \quad \text{at} \quad x = 0 \quad (A12a)$$

$$q D \frac{dn}{dx} = S n_q - J_o \quad x = d \quad (A12b)$$

J_o is the current produced in the region outside d . The current, J_p , is determined by

$$J_p = q D \frac{dn}{dx} \quad \text{at} \quad x = 0 \quad (A13)$$

The solution requires some algebraic manipulation and is as follows.

$$J_p = \frac{qaL}{1 - (aL)^2} [K_- + K_+ e^{-2ad}] \quad (A14)$$

$$+ J_0 / [\cosh(t/L) + \frac{SL}{D} \sinh(t/L)]$$

where $K_{\pm} = [(D/L \pm aLS) + (S \pm aD) \cosh(t/L) - \exp(\pm at) (S \pm aD) / \sinh(t/L)]$ (A15)

$$/[D/L \cosh(t/L) + S]$$

For the n^+ layer, a similar expression, J_n , is obtained. It is essentially Eqs. (A14) and (A15) with t replaced by $-t'$ where t' is the thickness of the n^+ region.

After multiplying by a factor that accounts for the optical absorption in the n^+ layer, the charge collection, $Q(\lambda)$ used in Eq. (A6) is just

$$Q(\lambda) = (J_p + J_n) / q \quad (A16)$$

Typical results are shown in Fig A2 where the efficiency is plotted as a function of thickness of the base thickness for various resistivities, diffusion lengths and back surface conditions.

REFERENCES

1. Five Year Research Plan, 1984-1988, Photovoltaics: Electricity from Sunlight, DOE/CE-0072, U.S. Department of Energy, May 1983.
2. F. Wald, Presented at the European Materials Research Society and to be published in J. Phys. Applique.
3. J.D. Zook, Appl. Phys. Letters, 37, 223 (1980).
4. C. Donolato, J. Appl. Phys., 54, 1314 (1983).
5. G.F.J. Garlick and A.H. Kachare, Appl. Phys. Letters, 36, 911 (1980).
6. J.I. Hanoka, R.O. Bell and B.R. Bathey, Proc. of Sym. on Electronic and Optical Properties of Polycrystalline or Impure Semiconductors and Novel Growth Methods, (Ed. by K.V. Ravi and B. O'Mara) p. 76, (The Electrochem. Soc. Pennington, N.J., 1980).
7. E.R. Weber, Appl. Phys. A20, 1 (1983).
8. S.M. Sze, "Physics of Semiconductor Devices", (Wiley-Interscience, New York, 1969), p. 30.
9. E. Schibli and A.G. Milnes, Mater. Science Engr., 2, 173 (1967).
10. Private communication, M.C. Cretella and B. Bathey.
11. B. Mackintosh, J.P. Kalejs, C.T. Ho and F. V. Wald, Proceedings of the Third CEC Photovoltaic Solar Energy Conf., Ed. W. Palz (Dordrecht, D. Reidel, 1980).
12. C.S. Fuller, "Defect Interactions in Semiconductors", Semiconductors, (Edited by N.B. Hannay), Academic Press, New York (1975).
13. J.G. Fossum and D.S. Lee, Solid State Electron., 25, 741 (1982).
14. J.G. Fossum, R.P. Mertens, D.S. Lee and J.F. Nijs, Solid State Electron. 26, 569 (1983).
15. A. Rhoatgi and P. Rai-Choudhury, IEEE Trans. Electron Dev., ED-31, 596 (1984).
16. Private communication M.C. Cretella.
17. D.L. Bowler and M. Wolf, IEEE Trans. Components, Hybrids and Manufacturing Tech., CHMT-3, 464 (1980).
18. ASTM Standard E-891, "Terrestrial Direct Normal Solar Spectral Irradiance for Air Mass 1.5".

19. D.E. Aspnes and A.A. Stunda, Phys. Rev. B, 27, 985 (1983).
20. F.A. Lindholm, J.A. Mazer, J.E. Dacis and J.I. Arreola, Solid State Electron., 23, 967 (1980).
21. R.O. Bell, Solid State Electron., 25, 175 (1982).
22. M.A. Green, IEEE Trans Electron. Dev., ED-31, 671 (1984).
23. M.A. Green, A.W. Blakers, J. Shi, E.M. Keller and S.R. Wenham, IEEE Trans. Electron. Dev., ED-31, 679 (1984).
24. M.B. Spitzer, S.P. Tobin and C.J. Keavney, IEEE Trans. Electron. Dev., ED-31, 546 (1984).
25. J.I. Hanoka, C.H. Seager, D.J. Sharp and J.K.G. Panitz, Appl. Phys. Letters, 42, 618 (1983).
26. M. Prince, J. Appl. Phys., 26, 534 (1955).
27. P.M. Dunbar and J.R. Hauser, A Theoretical Analysis of the Current-Voltage Characteristic of Solar Cells, Semiconductor Device Laboratory, North Carolina State University, Raleigh, NC, NASA Grant NGR 34-002-195, August 1975 and August 1976.
28. R.C. Y. Fang and J.R. Hauser, *ibid.*, September 1977 and January 1979.
29. J.J. Wysocki and P. Rappaport, J. Appl. Phys., 31, 571 (1960).
30. M. Wolf, IEEE Trans. Electron Devices, ED-27, 751 (1980).
31. J.B. Gunn, J. Electron. Contr., 4, 17 (1958).

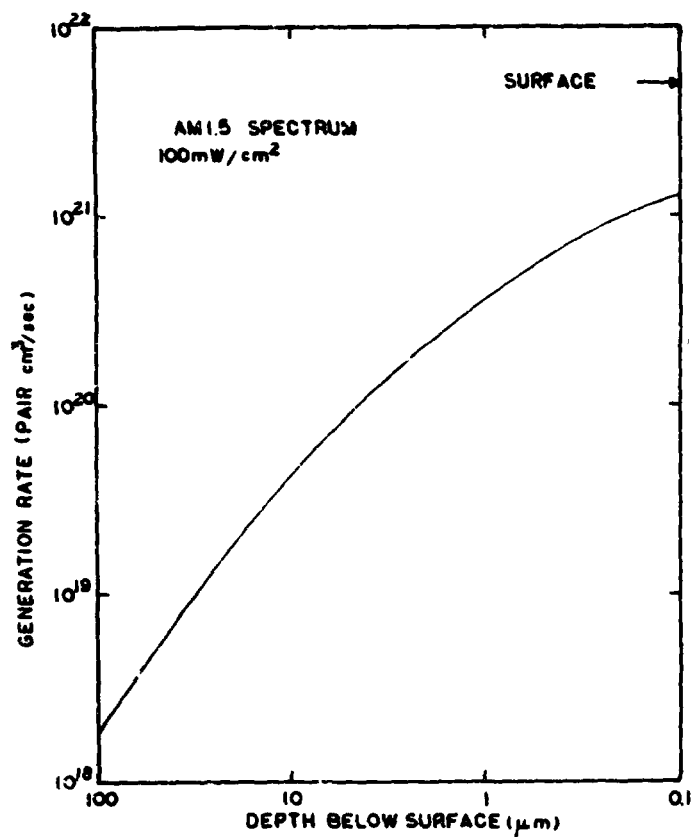


Fig. 1. Charge generation rate as a function of depth below the surface of the standard AM1.5 spectrum.

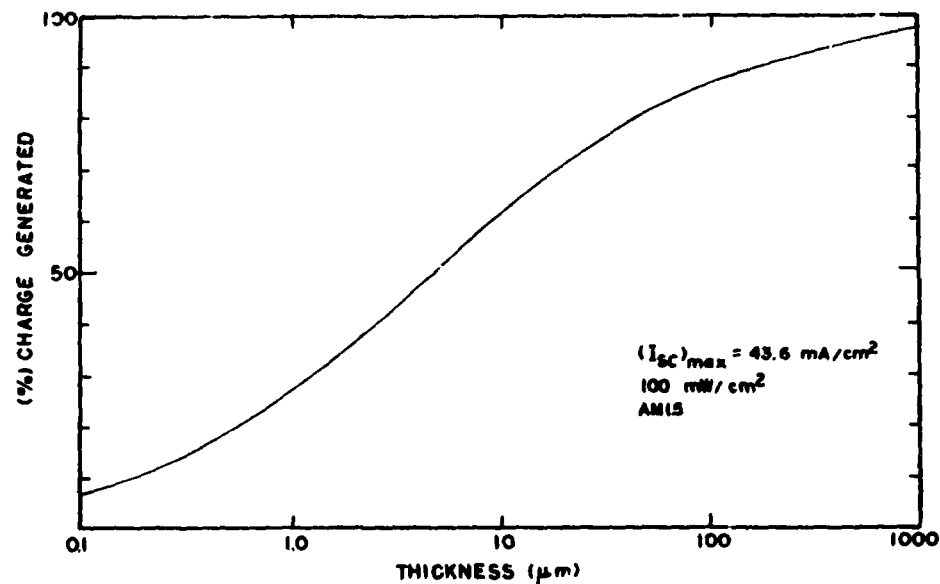


Fig. 2. Relative number of hole-electron pairs generated between the surface and depth t . The curve is normalized with respect to the number of photons being absorbed in a thick piece of silicon.

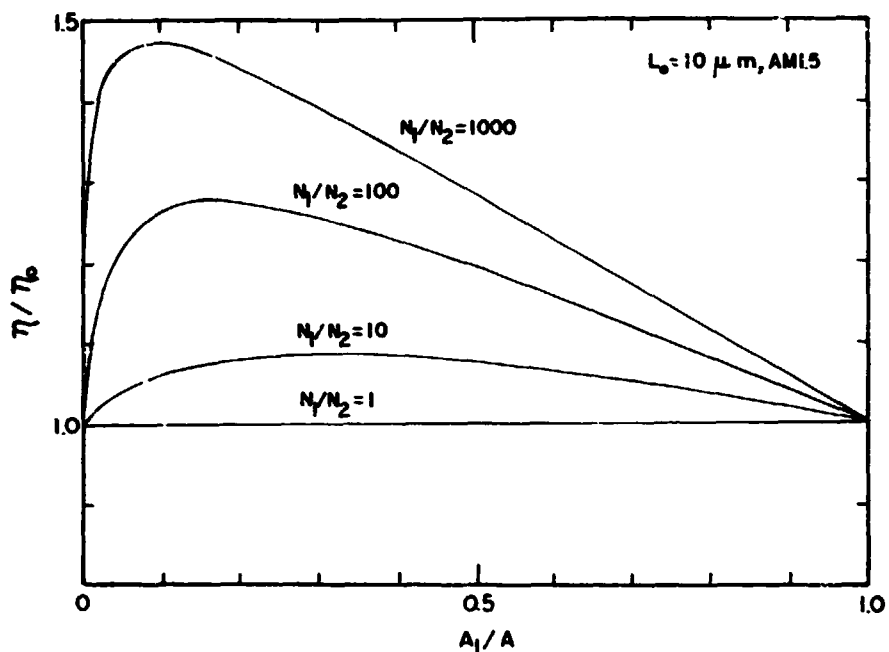


Fig. 3. Normalized solar cell efficiency as a function of poor area for different relative numbers of recombination centers.

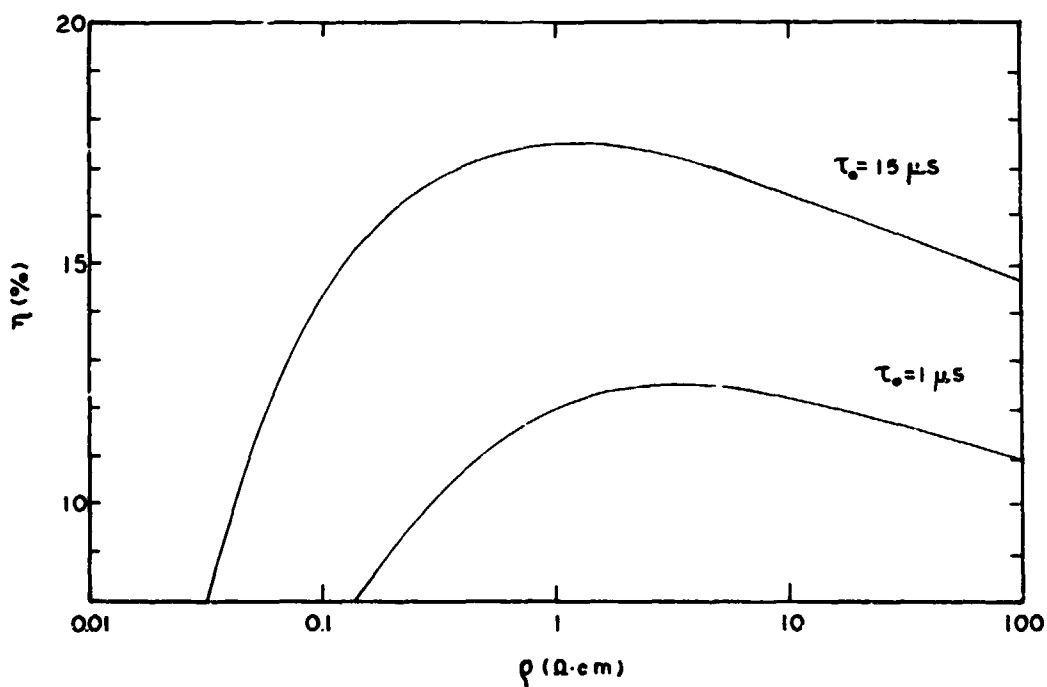


Fig. 4. Efficiency of a solar cell as a function of resistivity whose minority carrier lifetime varies as given by Eq. (2) in the text.

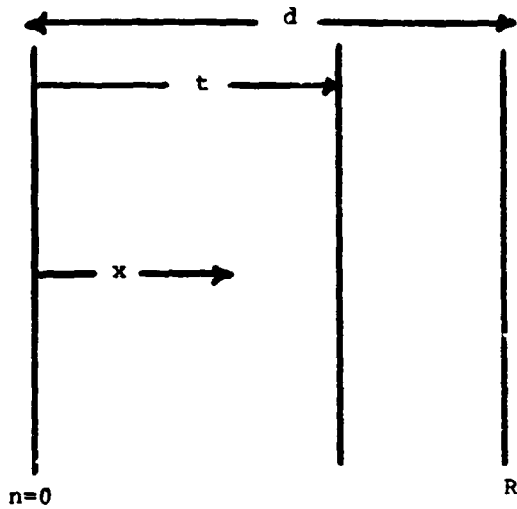


Fig. A1. Geometry used to calculate solar cell performance. The photons are incident on the left-hand side.

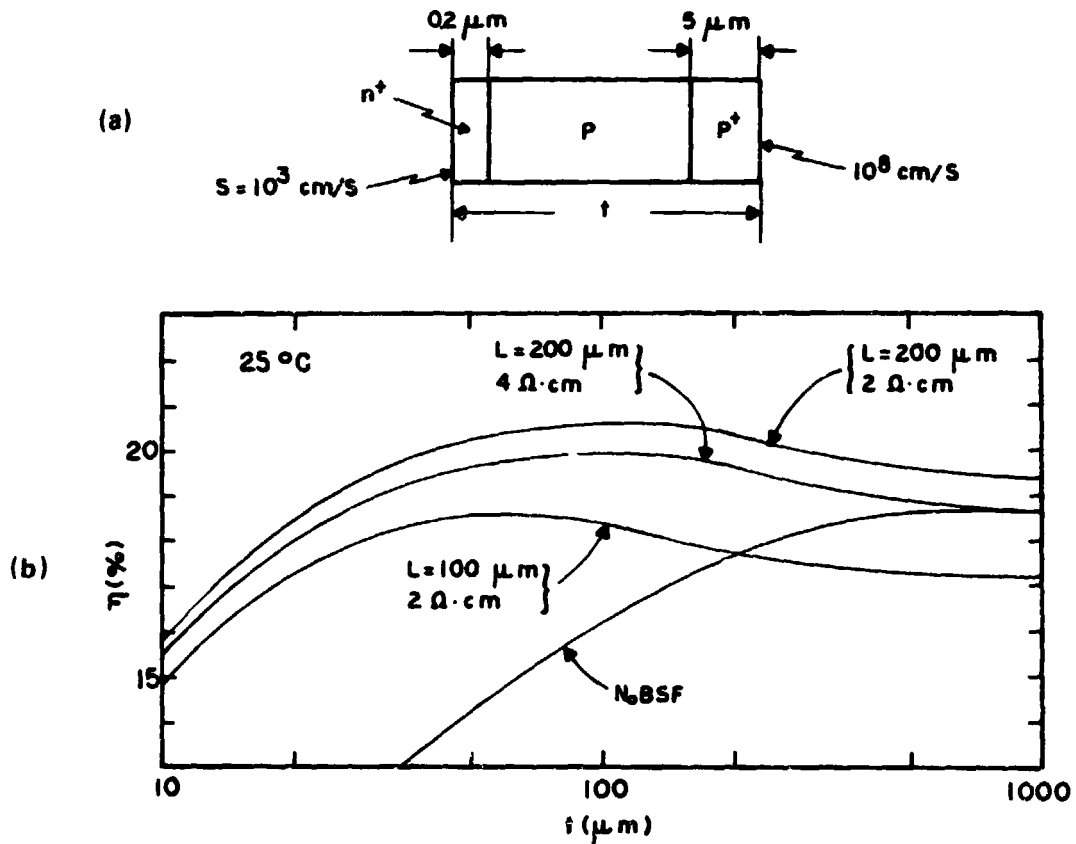


Fig. A2. (a) Physical dimensions and electrical parameters used in calculating solar cell performance. (b) Calculated efficiency of solar cell as a function of total sample thickness for various diffusion lengths and resistivities. The curve labeled $N_0 \text{ BSF}$ is the result with no back surface field being present.

DISCUSSION

DYER: Is there still a preferred orientation of the grain structure in these sheet structures, and is that [110], the surface of it?

BELL: The surface tends to be OK, the orientation is a {211}. Correction: it tends to be.

DYER: What about the surface?

BELL: I believe it is close to [110], we call it an equilibrium structure. As you grow, no matter what orientation you start with, you are growing to a certain distance. It essentially tends to become {211}.

DYER: How close is that to <110>? Is it plus or minus 10 degrees, five degrees----?

BELL: Ten or 20 degrees is the type of thing that one sees.

QUESTION: You mentioned the possibility of silicon carbide particles shunting the junction. Have you run into a situation where a grid line hits a particle?

BELL: Yes, I should mention that in the unfortunate event that a grid line hits a particle, the cell is shorted. Luckily, if you only have 5% good coverage and something less than 1 per cube per cm^2 , the probability is fairly low.

QUESTION: As you go to larger cells the probability of that will increase.

BELL: That's right, but even when we are talking about 50 cm^2 cells it is well under 0.1%, I really don't know what the statistics are but it is quite low.

LESK: Ast has written several reports in which he uses a 1200°C anneal on EFG materials, passivates the grain boundaries at this location. The results in his reports are quite striking. You haven't mentioned that hydrogen passivation. I wonder if you might comment on which one works best.

BELL: We find, certainly, that the heat treatments that one gives to the material can have fairly dramatic effects on its behavior. We have found that if one goes to a high temperature, like to 1200°, for a fairly short period of time - 10 minutes to a half an hour, something like that -- often one finds an improved performance. The problem is, we are dealing with a fairly complicated situation; material grown from a quartz crucible and material grown from a carbon crucible often have somewhat different behavior. Although people from Mobil and others have had a lot of theories and ideas on what is going on, in my mind there is no clear picture. There is a lot of interaction going on.

QUESTION: I would like to ask a question about hydrogen passivation. Are

these passivating the grain boundaries, mainly, or also impurities and defects? How do you apply it in the high-temperature form, atomic form or cosmic form?

BELL: I really wish I had another slide to show the grain. Jack Hanoka is going to discuss the work that we have done with hydrogen passivation; I'll just say that it does passivate the grain boundaries and other parameters, but we will let Jack talk about the details.